New Aspects on the Frequency Splitting and Bifurcation Phenomena in Wireless Power Transfer Systems

Mihai Iordache*, Andrei Marinescu†, Ioana-Gabriela Sîrbu‡, Lucian Mandache‡, Dragoş Niculae* and Lavinia Iordache*

* Politehnica University of Bucharest, Faculty of Electrical Engineering, Bucharest, Romania, mihai.iordache@upb.ro, dragos.niculae@upb.ro, laviniabobaru@gmail.com

† INCD - ICMET, Craiova, Romania, amarin@icmet.ro

‡ University of Craiova, Faculty of Electrical Engineering, Craiova, Romania, osirbu@elth.ucv.ro, lmandache@elth.ucv.ro

Abstract - **This paper focuses on the frequency splitting and bifurcation phenomena that appear in the wireless power transfer systems. These two phenomena are analyzed for different possible configurations of the magnetically coupled circuits of the system, through electric circuit methods and mathematical calculus. Considering two printed spiral coils with similar geometrical properties, the study started with a calculus of the splitting frequency. It was made for the series-series connection, but also for series-parallel, parallel-series and parallel-parallel connections. The graphical representations of the load voltage as function of the frequency revealed that this phenomenon is visible only for the series-series and series-parallel connections; even if one or two peaks appear in all cases they are not directly connected to the frequency splitting phenomena, respectively to the spitting factor. The bifurcation phenomenon is analyzed starting from the bifurcation equation defined for the input admittance of the wireless power transfer system. The four types of configurations are analyzed from the graphical representations of the imaginary part of the admittance as function of the frequency. Because an important factor in the frequency splitting and bifurcation phenomena appearance is the ratio between the input resistance and the load resistance, in the last part of the paper the splitting coupling factor as function of the input resistance - load resistance ratio is depicted. The paper brings new contributions in the field through a comparative study on the frequency splitting and bifurcation phenomena for all the four types of configuration of the wireless power transfer systems. Through mathematical calculations, formulas for estimating the frequency (angular frequency) of occurrence of each phenomenon are obtained. The results are validated by comparative simulations related to a system of identical spiral coupled coils. The results of the analysis were commented comparatively and some conclusions could be drawn.**

Keywords: *inductive power transmission, circuit analysis, equivalent circuits, splitting and bifurcation phenomena.*

I. INTRODUCTION

Frequency splitting and bifurcation phenomena were often mentioned in the context of the studies, analyzes and applied researches that had as subject the wireless power transfer (WPT) systems [1–19]. Many researchers have approached tangentially or deeply this topic, trying to explain the theoretical and practical consequences of the occurrence of these phenomena, with their advantages and disadvantages. The researches have focused mostly on the series-series connection, but lately other types of connections were analyzed, too in order to identify the best option.

It is already known now that the frequency splitting phenomenon appears at the magnetically coupled circuits when the coupling factor exceeds a certain critical value called the splitting factor. It is characterized by the fact that in the curves of some output quantities (load voltage, active power load, etc.) represented as functions of the frequency there is not a single point of maximum (peak), but two. In most of the cases they have different values (the first peak is higher than the second one). The regions of the curve bounded by the two peaks are called in literature [2, 3, 12, 18]: the low frequency region, the stagger tuning region and the region of high frequencies. The part of the curve situated between the two peaks (the stagger tuning region) proved to be useful to maintain constantly the voltage transfer factor in the applications characterized by variable load or by inconstant distance between the coils [19]. The high frequency region is preferred for the output voltage controlling [2, 5, 13]. The WPT system behavior under the frequency splitting phenomenon should be well known in order to ensure an optimum power transfer from the source circuit to the receiver circuit. Thus it was observed that the energy transfer is much more efficient if the two circuits operate at the same frequency (resonant circuits) [7 – 9, 11].

If the frequency splitting phenomenon characterizes the output quantities of the WPT system, the frequency bifurcation phenomenon is related to the input quantities of the system (either input impedance or input admittance). Each bifurcation angular frequency is an operating mode of the system. These modes could be stable or unstable. Each operating mode has its own transfer characteristics [18].

This paper has proposed to explore new aspects concerning these two phenomena that may occur in the WPT systems. For the frequency splitting phenomenon the attention was concentrated on finding the splitting frequencies / angular frequencies through a mathematical calculus. The finding of the extreme points was not made for the load active power - frequency curve as in other previous papers [18], but for another output quantity, i.e. output voltage (load voltage). As for the frequency bifurcation phenomenon, the analysis was centered on the variation with the frequency of the imaginary part of the input admittance, and not of the input impedance as it is treated generally in the literature. The analyses were made for all the possible configurations of the WPT system: series-series, series-parallel, parallel-series, and parallel-parallel. Finally the paper presents some aspects regarding the variation of the splitting coupling factor as function of the ratio between the load resistance and the input resistance. The comparative graphical representations made in each case have revealed the different behavior of the system for different configurations and for various values of the coupling factor. Some important conclusions were drawn in the end of the work.

II. System Parameters

The system used for the analysis consists of two identical printed spiral coils having the inner radius r_i = 3.3 mm, the coil width l = 22.8 mm, the distance between two consecutive turns (the pitch) p = 1.2 mm, the copper section area s = 1.2x0.8 = 0.96 mm^2, the coil mean radius $r_m = r_i + l/2$ = 14.4 mm and the number of turns N = 10 (Fig. 2) [18]. A part of its electrical parameters could be determined on the basis of some approximate formulas [20]. However, in order to estimate as accurately as possible all the parameters of interest we preferred to make a numerical calculation using the program ANSOFT EXTRACTOR Q3D [21]. Choosing a distance between coils d = 50 mm and the frequency f = 5 MHz we obtained: C_1 = 1.1785 nF; C_2 = 1.18 nF; L_1 = 2.3172 μH; L_2 = 2.3098 μH; M = 0.8775 μH; $R_5 = R_{L1}$ = 0.5971 Ω and $R_6 = R_{L2}$ = 0.57186 Ω. These parameters allowed obtaining the equivalent circuit of the system in the parallel-series (*ps*) configuration (Fig. 1). On its base the other connection types of the equivalent diagram can be obtained relatively easily: series-series (*ss*), series-parallel (*sp*) and parallel-parallel (*pp*). The source has the rms value E_i = 15 V and the internal resistance $R_7 = R_i$ = 1.5 Ω, and the load has the resistance $R_8 = R_L$ = 30 Ω (a resistive load).

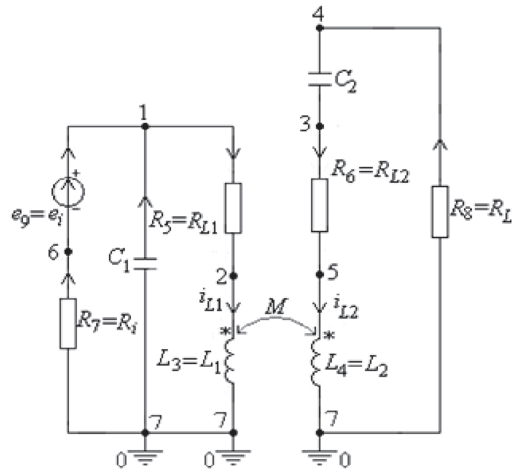

Fig. 1. The equivalent circuit of a WPT system - configuration *ps*.

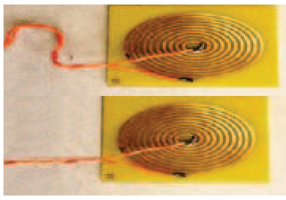

Fig. 2. Printed coils.

III. The Analysis of the Frequency Splitting Phenomenon

The frequency splitting phenomenon is related to the appearance of two peaks instead of one in the dependence curve of an output quantity (active power load, load voltage, the absolute value of the voltage transfer factor, etc.) on the frequency, when the coupling factor k exceeds a certain critical value called *frequency splitting coupling factor*, k_{split}. Therefore k_{split} is the maximum value of the coupling factor up to which the frequency splitting phenomenon does not appear [18]. Sometimes the two peaks have almost the same value, but there are cases when the first peak has a value higher than the second one. In the coupled modes theory the frequency corresponding to the first peak is called *the odd splitting frequency* and the frequency corresponding to the second maximum value is called *the even splitting frequency* [2, 13, 18].

As output quantity in the study of the frequency splitting phenomenon we considered further the load voltage U_L. The condition for finding the extreme points of the load voltage - frequency (angular frequency) curve is

$$\frac{\partial U_L}{\partial \omega} = 0 \tag{1}$$

named *the splitting equation* [2, 13].

The points of maximum will correspond to some roots of this equation.

Obviously the equation (1), where the unknown is the angular frequency ω, has its coefficients dependent on the circuit parameters (i.e. capacitances, inductances and resistances, as in Fig. 1) and also on the coupling factor k.

As a remark we could notice that its free term has always a negative value. Also, the final structure of (1) allows the replacement of the term ω^2 with y. Because the load voltage - angular frequency curve must have a single peak, the equation (1) must have only one real root.

Equation (1) takes different forms depending on the connection type considered, as it will be seen below.

A. Series-Series Connection

The equation (1) becomes a 4th degree equation in y ($y = \omega^2$) in the form [18]

$$ay^4 + by^2 + cy + d = 0\,, \tag{2}$$

where a, b, c and d depend on the electrical parameters of the circuit, and $d < 0$.

Because only one maximum is wanted, the equation (2) must have three equal real roots: $y_1 = y_2 = y_3 = y_e$ [4, 18].

Thus, using the Vieta's formulas [22], we obtained the system:

$$\begin{cases} 3y_e + y_4 = 0 \Rightarrow y_4 = -3y_e \\ 3y_e(y_e + y_4) = b/a \\ y_e^{\,2}(y_e + 3y_4) = -c/a \\ y_e^{\,3} y_4 = d/a \end{cases} \quad (3)$$

from which we obtained

$$y_e = -\frac{3c}{4b} \text{ and } 3\left(\frac{3c}{4b}\right)^4 + \frac{d}{a} = 0. \quad (4)$$

In order to obtain the coupling factor k_{split} that determines a single peak for the load voltage U_L curve, from (4) we obtained the solution:

$$\omega_{split\_ss} = \sqrt{\left|-\frac{3c}{4b}\right|}, \quad (5)$$

that depends on the coefficients of the equation (2).

B. Parallel - Series Connection

In this case the general equation (1) takes the form

$$ay^4 + by^3 + cy + d = 0, \quad (6)$$

with $d < 0$.

A condition similar to the previous one is put also in this case (three real roots equal to y_e), to obtain a single maximum. Vieta's relations [18, 22] lead now to the conditions:

$$y_e = -\frac{b}{2a},\ b^3 + 4a^2c = 0 \text{ and } b^4 + 16a^3d = 0. \quad (7)$$

From (7) we searched for a solution in order to find a minimum value of the coupling factor k_{split} that ensure a single maximum for the load voltage U_L curve.

By replacing the coefficients in the last two relations (7) by their expressions (functions of electric parameters and coupling factor $k = M/\sqrt{L_1 \cdot L_2}$) two equations in k are obtained. The common solution of these two equations that determines a minimum coupling factor has the expression [18]

$$\omega_{split\_ps} = \sqrt{\left|-\frac{b}{2a}\right|}. \quad (8)$$

C. Series - Parallel Connection

This case offers, from (1), an equation similar to (6), obviously with different expressions for its coefficients *a*, *b*, *c* and *d*. So the solution (8) is valid also for this connection.

D. Parallel - Parallel Connection

The equation (1) becomes in this case a 4th degree equation in *y* in the form [18]

$$ay^4 + by^3 + cy^2 + d = 0, \quad (9)$$

where $d < 0$.

Similarly the condition of having three equal positive real roots together with the Vieta's formulas [18, 22] lead to the relations

$$y_e = -\frac{3b}{8a},\ 9b^2 - 32ac = 0 \text{ and } 27b^4 + 8^4 a^3 d = 0 \quad (10)$$

So the common solution of the last two equations (10) that determines a minimum coupling factor has the expression

$$\omega_{split\_pp} = \sqrt{\left|-\frac{3b}{8a}\right|}. \quad (11)$$

As a general remark we could found that formally the equations obtained for each case and thus their solutions are similar to those in [18] where the analysis was done for the output quantity P_L (load active power). Of course, the equation coefficients have completely different expressions here, but they depend also on the electrical parameters of the circuits and on the coupling factor.

E. Comparative Results

The four types of connection of the WPT system were analyzed further in a comparative manner. The system to be analyzed has the geometrical and electrical parameters presented in section II. For this system the following parameters were also calculated: the resonance angular frequency $\omega_0 = \frac{2}{\sqrt{(C_1 + C_2)(L_1 + L_2)}} = 1.9145 \cdot 10^7$ rad/s; the resonance frequency f_0 = 3.0486 MHz, and the coupling factor corresponding to the normal operation of the system $k_n = M/\sqrt{L_1 \cdot L_2} = 0.3793$.

With these values of the parameters the variation curves of the load voltage U_L as function of the frequency, for different values of the coupling factor *k*, were depicted. Thus Fig. 3 presents the load voltage variations as function of the frequency for the four types of connection:

• *ss* connection and six values of the coupling factor: k_1 = 0.1, $k_c = 1/\sqrt{Q_1 \cdot Q_2}$ = 0.181 (where $Q_1 = (\omega_0 \cdot L_1)/(R_{L1} + R_i)$ and $Q_2 = (\omega_0 \cdot L_2)/(R_{L2} + R_L)$ are the quality factors of the two inductively coupled circuits), k_n = 0.3793, k_{split} = 0.5035, k_2= 0.6 and k_3 = 0.8 (Fig. 3 (a));

• *sp* connection and seven values of the coupling factor: $k_c = 1/\sqrt{Q_1 \cdot Q_2}$ = 0.024724 (where $Q_1 = (\omega_0 \cdot L_1)/(R_{L1} + R_i)$ and $Q_2 = (\omega_0 \cdot L_2)/R_{L2}$ are the quality factors of the circuits), k_1 = 0.15, k_n = 0.3793, k_2 = 0.45, k_{split} = 0.6201, k_3 = 0.8 and k_4 = 0.9 (Fig. 3 (b));

• *ps* connection and seven values of the coupling factor: $k_c = 1/\sqrt{Q_1 \cdot Q_2}$ = 0.09647 (where $Q_1 = (\omega_0 \cdot L_1)/R_{L1}$ and $Q_2 = (\omega_0 \cdot L_2)/(R_{L2} + R_L)$ are the quality factors of the circuits), k_1 = 0.15, k_2 = 0.25, k_n = 0.3793, k_3 = 0.6, k_4 = 0.75 and k_5 = 0.9 (Fig.3 (c)), and

• *pp* connection and seven values of the coupling factor: $k_c = 1/\sqrt{Q_1 \cdot Q_2}$ = 0.0132 (where $Q_1 = (\omega_0 \cdot L_1)/R_{L1}$ and $Q_2 = (\omega_0 \cdot L_2)/R_{L2}$ are the quality

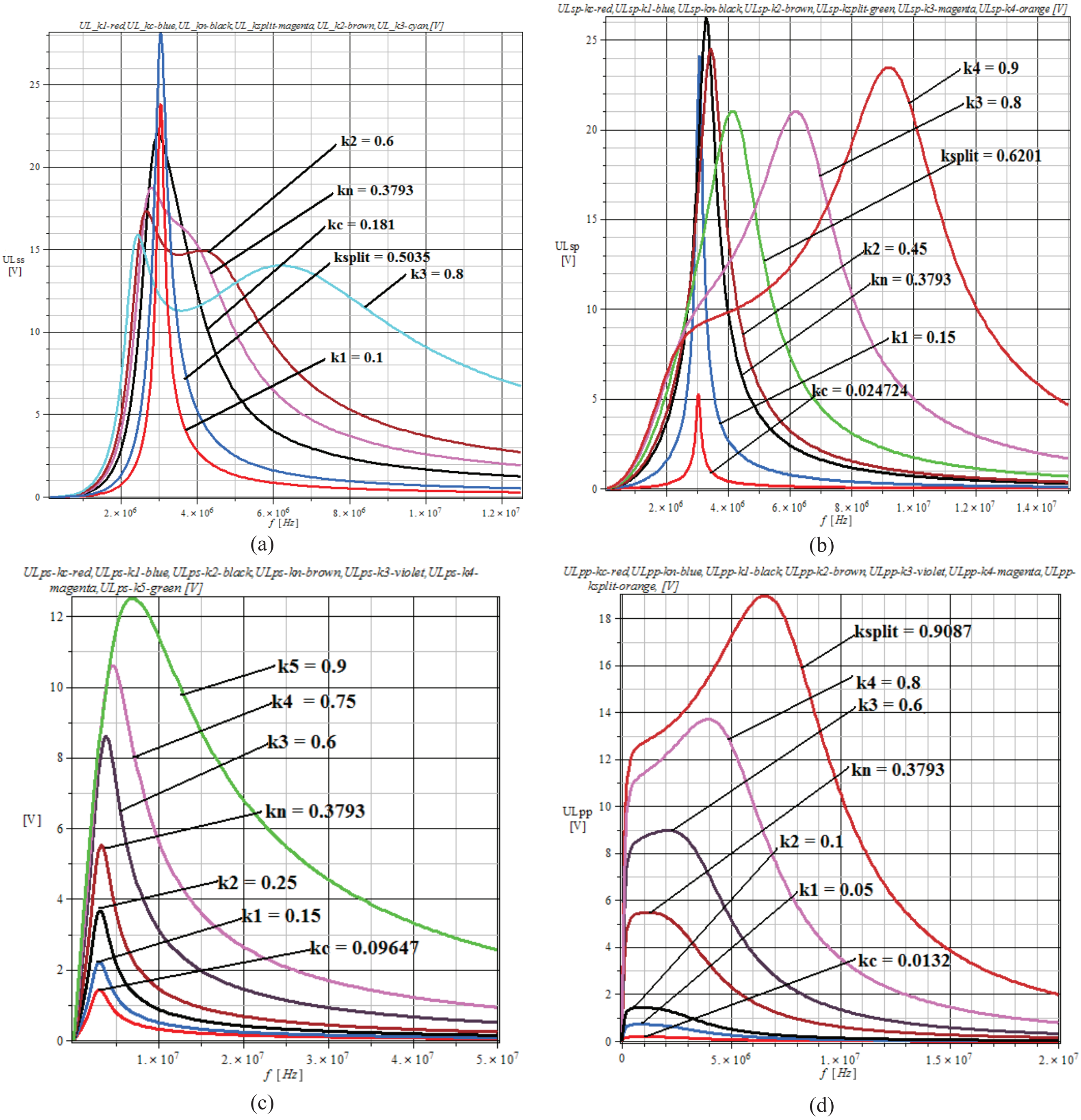

Fig. 3. Load voltage U_L variations as function of the frequency *f* : (a) *ss* connection; (b) *sp* connection; (c) *ps* connection; (d) *pp* connection.

factors of the circuits), $k_1 = 0.05$, $k_2 = 0.1$, $k_n = 0.3793$, $k_3 = 0.6$, $k_4 = 0.8$ and $k_{split} = 0.9087$ (Fig.3 (d)).

The curves shapes analysis has shown that the frequency splitting phenomenon is visible for the *ss* and *sp* connections (Figs.3 (a) and (b)). In these cases for the values of $k > k_{split}$ the load voltage - frequency curves have two peaks. When $k = k_{split}$, the three extreme frequencies are equal and only one peak is obtained. For $k \leq k_{split}$ the load voltage - frequency curves have a single maximum point. In fact $k < k_{split}$ corresponds to the so-called frequency splitting - free region [18]. For the *ps* and *pp* connections (Figs. 3 (c) and (d)) the frequency splitting phenomenon is not noticeable on the $U_L - f$ curves. At the *ps* connection only one peak is obtained for every value of the coupling factor. As for the *pp* connection a change in the shape of the curve is remarked, but it is not directly connected to the value of the k_{split} (the curve shape is changed even for values of *k* lower than k_{split}). However the frequency splitting phenomenon exists also at the *ps* and *pp* connections and it could be seen in the curves of the power transfer efficiency η_{21} as function of the frequency [2–4, 17, 18].

In Figs. 4 (a), (b), (c) and (d) the 3D variations of the load voltage U_L versus frequency *f* and magnetic coupling factor *k* - corresponding to the four connections of the magnetically coupled coils system - are presented.

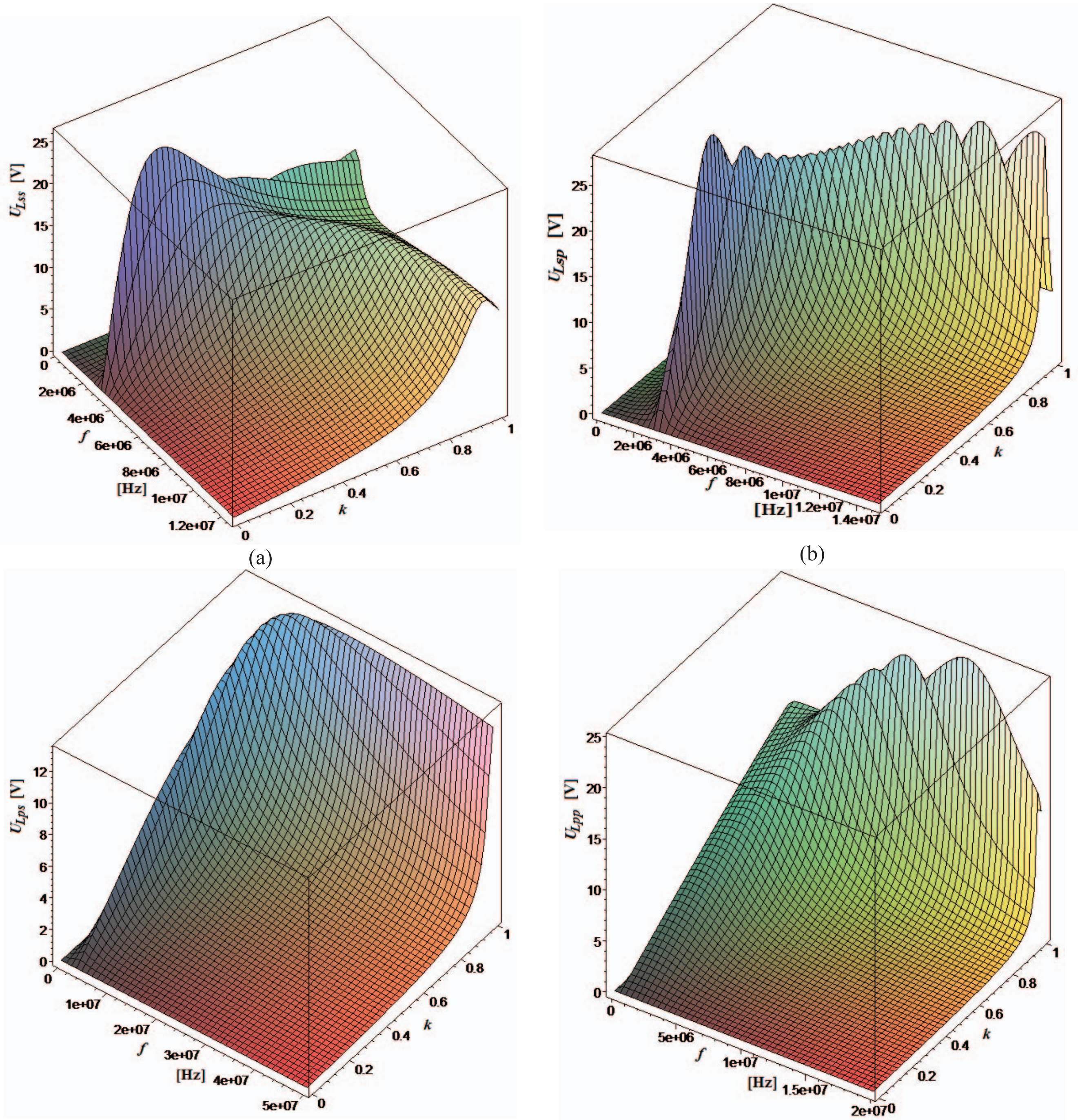

(a) (b) (c) (d)

Fig. 4. 3D load voltage U_L variations as function of the frequency f and of the magnetic coupling factor k : (a) *ss* connection; (b) *sp* connection; (c) *ps* connection; (d) *pp* connection.

They concentrate the results arising from the analysis of the comparative curves in Fig. 3.

IV. THE ANALYSIS OF THE FREQUENCY BIFURCATION PHENOMENON

The bifurcation phenomenon is related to the input characteristics of the wireless power transfer systems. Usually the input impedance is used as reference parameter [3, 17, 18], but also the input admittance could be considered.

Starting from the bifurcation equation defined in the literature [1-18] and using as input parameter the admittance, the bifurcation equation is in this case:

$$\mathrm{Im}(\underline{Y}_{in}) = 0\,, \qquad (12)$$

where $\underline{Y}_{in}$ is the input complex admittance of the WPT system. By making the substitution $\omega^2 = x$ in (12), a 3rd degree equation in x is obtained, of form:

$$a_3 x^3 + a_2 x^2 + a_1 x + a_0 = 0\,, \qquad (13)$$

where a_3, a_2, a_1 and a_0 are the coefficients of the equation. They depend on the values of the parameters of the two resonant circuits.

It can be demonstrated that the bifurcation equation (12) can be brought to a form (13) for each of the four types of possible connections of the two circuits [4, 17, 18].

In order to obtained the value of the coupling factor k when the bifurcation phenomenon starts we put the condition that all the (three) roots must be equal and real, according to Vieta's formula [2, 4, 16–18, 22]. Thus the following relations must be accomplished:

$$3\left(-\frac{a_2}{3a_3}\right)^2-\frac{a_1}{a_3}=0$$

$$\left(-\frac{a_2}{3a_3}\right)^3+\frac{a_0}{a_3}=0 \qquad (14)$$

$$\omega_{bif}=\sqrt{x}=\sqrt{-\frac{a_2}{3a_3}}.$$

It can be noticed that these formula are similar to those obtained starting from the bifurcation equation in the complex impedance [18].

The literature offers an analytical approximate solution for the equations (14), obtained for the *ss* connection [2, 4, 16 – 18]:

$$k_{bif}=(1/Q_c)\cdot\sqrt{1-1/(4Q_c^2)}\,, \qquad (15)$$

where $Q_c=\sqrt{Q_1\cdot Q_2}$, $Q_1=(\omega_0 L_1)/(R_{L_1}+R_i)$, and $Q_2=(\omega_0 L_2)/(R_{L_2}+R_L)$. k_{bif} is named the coupling coefficient of the bifurcation. Also a factor $k_c=1/Q_c$ could be defined. Equivalent formulae could be obtained also for the other three types of connection.

The curves of the imaginary part of the input admittance $\underline{Y}_{in}$ as function of the frequency f for the system of two magnetically coupled circuits having the parameters presented in section II are represented in Fig. 5, for the four types of connection:

• *ss* connection and six values of the coupling factor, $k_1 = 0.1$, $k_c = 0.181$, $k_n = 0.3793$, $k_{split} = 0.5035$, $k_{bif} = 0.64045$ and $k_3 = 0.8$ (Fig. 5 (a));

• *sp* connection and eight values of the coupling factor: $k_c = 0.024724$, $k_1 = 0.15$, $k_n = 0.3793$, $k_3 = 0.45$, $k_{split} = 0.6201$, $k_{bif\,1} = 0.62013$, $k_{bif\,2} = 0.794$ and $k_4 = 0.9$ (Fig.5 (b));

• *ps* connection and seven values of the coupling factor: $k_c = 0.09647$, $k_1 = 0.15$, $k_2 = 0.25$, $k_n = 0.3793$, $k_3 = 0.6$, $k_4 = 0.75$ and $k_{bif} = 0.95125$ (Fig.5 (c)), and

• *pp* connection and seven values of the coupling factor $k_c = 0.0132$, $k_1 = 0.05$, $k_2 = 0.1$, $k_n = 0.3793$, $k_3 = 0.6$, $k_{bif} = 0.797$ and $k_{split} = 0.9087$ (Fig.4 (d)).

The variation range of the frequency for $k > k_{bif}$ is called the bifurcation region, while the variation range when $k < k_{bif}$ is called the bifurcation - free region. In the bifurcation region the bifurcation equation have two positive real roots: the bigger one is called the big bifurcation angular frequency and the smaller one is named the small bifurcation angular frequency [18].

By analyzing the curves of the input admittance as function of the frequency from Figs. 5 (a) - (d) a different behavior is remarked for the four types of connection. The *ss* connection presents a strong reduction of the negative peak for the coupling factors bigger than k_{bif} (in the bifurcation region). At the *sp* connection, if $k > k_{bif}$, a displacement of the zero crossing point of the curve is noticed, from the resonance frequency $f_0 = 3.0486$ MHz towards frequencies even three times bigger (if k is about 0.9). In the *ps* connection no difference is remarked at the coupling factor variation, so the bifurcation phenomenon is not visible for this type of graphical representation. This phenomenon is again highlighted at the *pp* connection, when for the coupling factors higher than k_{bif} two extreme points appear.

It should be noted that the studies in the domain of frequency splitting and bifurcation phenomena have shown that a special influence on these phenomena has the ratio between the input resistance R_i and the load resistance R_L and also the ratio between the transmitter inductance L_1 and the receiver inductance L_2 [18]. This is why Figs. 6 (a) and (b) present the variation of the splitting coupling factor k_{split} as function of the ratio $\alpha = R_L / R_i$, for two of the four possible connections of the magnetically coupled circuits: *ss* connection and *sp* connection.

Fig. 6 (a) shows that at the *ss* connection by varying the ratio $\alpha = R_L / R_i$ between 0 and 40 - all the other parameters of the two resonators remaining constant - the splitting coupling factor k_{split} increases continuously between 0.04 and 1.0. Fig. 6 (b) highlights that by changing the ratio α between 0 and 100, at the *sp* connection, the other parameters remaining the same, the splitting coupling factor decreases from 1.0 to 0.06. These variations of the splitting factor confirm once again that at the connections *ss* and *sp* the frequency splitting phenomenon is present. Not the same thing can be said on the other two connections, *ps* and *pp*. The curves of α (not represented here) presented only very small variations of the k_{split}, fact that confirms the nonappearance of a clear splitting phenomenon at these connections.

V. CONCLUSION

This work brings new aspects on the frequency splitting and bifurcation phenomena, that are present in the wireless power transfer systems. The all four types of connection were analyzed for the system of two magnetically coupled circuits: series-series, series-parallel, parallel-series and parallel-parallel.

The frequency splitting phenomenon focused on the load voltage – frequency characteristic, using thus another output quantity that the usual one (the load active power). The calculus made using the electric circuit theory and algebraic equations is finalized with some useful formulae that permit the calculation of the splitting frequencies for each of the four connection types. These relations, compared with those obtained for the load active power, revealed some important similarities.

The study of the frequency bifurcation phenomenon was made for the input admittance, and not for the impedance; similarities were found here, too.

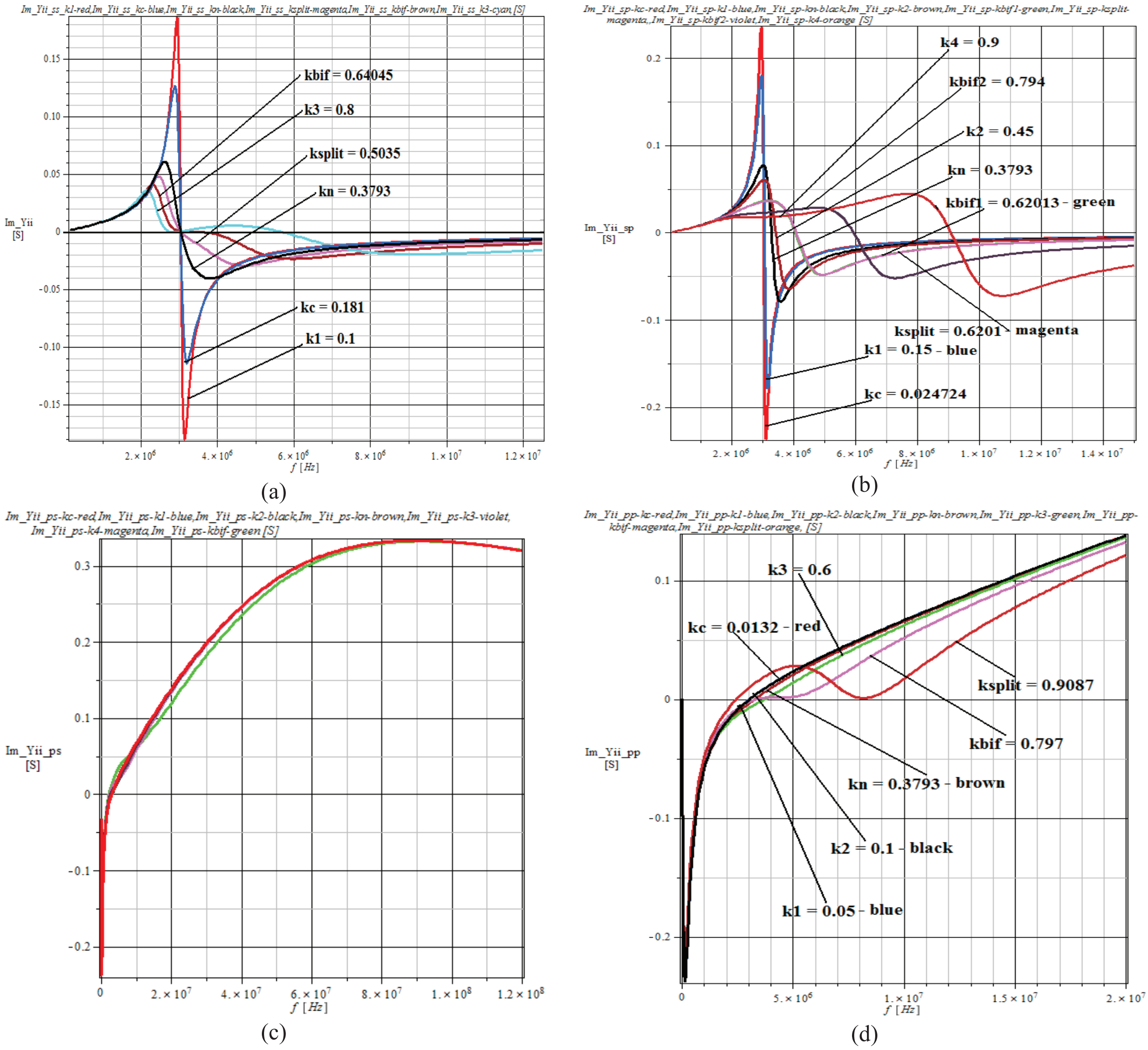

Fig. 5. $\underline{Y}_{in}$ imaginary part variations as function of the frequency f: (a) *ss* connection; (b) *sp* connection; (c) *ps* connection; (d) *pp* connection.

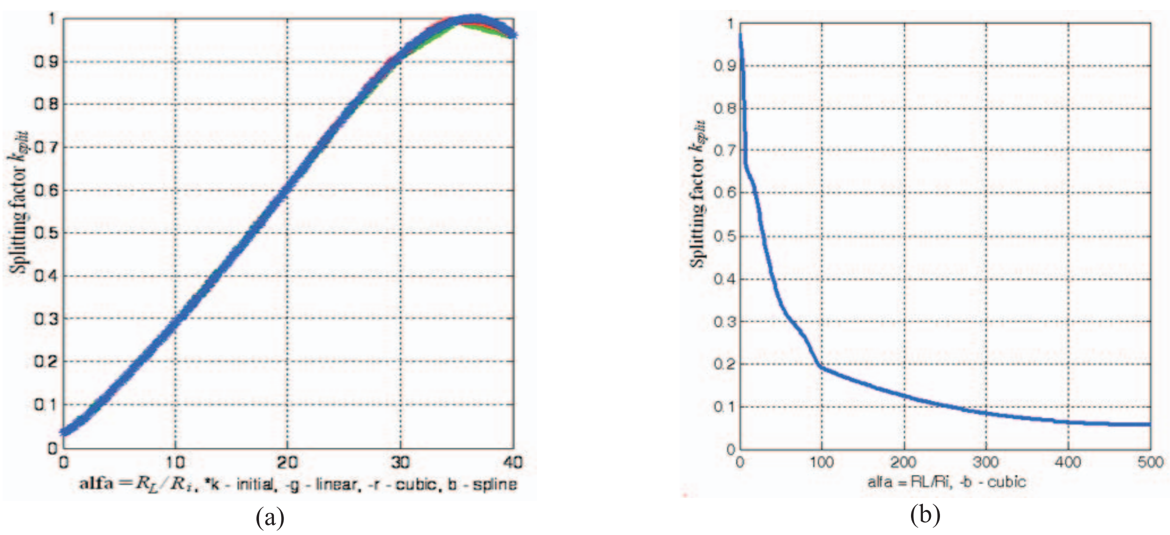

Fig. 6. Coupling coefficient k variations as function of the ratio $\alpha = R_L / R_i$: (a) *ss* connection; (b) *sp* connection.

For each phenomenon the results included also graphical representations, very suggestive, presented comparatively for different values of the coupling factor and for the four alternatives of connection of the circuits. The paper provides also some clues on how it could be estimated, with a rather good accuracy, the limit value of the coupling factor that decides the appearance or the non-appearance of any of the two phenomena. The study on the variation of the splitting coupling factor as function of the load resistance - input resistance ratio ends this work.

The studies presented in this work completes the previous made and published analyzes in the domain of wireless power transfer systems, bringing new and useful information for the researchers and the designers of such systems.

Received on July 29, 2016
Editorial Approval on November 18, 2016

REFERENCES

[1] A. Kurs, A. Karalis, R. Moffatt, J. D. Joannopoulos, P. Fisher, and M. Soljacic, "Wireless power transfer via strongly coupled magnetic resonances", *Science*, vol. 317, no. 5834, pp. 83–86, Jul. 2007.

[2] W. Q. Niu, J. X, Chu, W. Gu, and A. D, Shen, „Exact analysis of frequency splitting phenomena of contactless power transfer systems", *IEEE on CAS – 1*, Vol. 60, No. 6, pp. 1670 – 1677, June 2013.

[3] C. S.Wang, G. A. Covic, and O.H. Stielau, "Power transfer capability and bifurcation phenomena of loosely coupled inductive power transfer systems", *IEEE Trans. Ind. Electron*., vol. 51, no. 1, pp. 148–157, Feb. 2004.

[4] M. Iordache, D. Niculae, L. Iordache (Bobaru), and L. Mandache, „Circuit analysis of frequency splitting phenomena in wireless power transfer systems", *Proc. of the 9th International Symposium Advanced Topics in Electrical Engineering – ATEE'15*, May 7-9, 2015, Bucharest, Romania, pp. 146 - 151.

[5] M. W. Baker and R. Sarpeshkar, "Feedback analysis and design of RF power links for low-power bionic systems", *IEEE Trans. Biomed. Circuits Syst*., vol. 1, no. 1, pp. 28–38, March 2007.

[6] A. Karalis, J. D. Joannopoulos, and M. Soljačić, "Efficient wireless non-radiative mid-range energy transfer", *Annals of Physics*, Vol. 323, pp. 34-48, January 2008.

[7] T. Imura and Y. Hori, "Maximizing air gap and efficiency of magnetic resonant coupling for wireless power transfer using equivalent circuit and Neumann formula", *IEEE Trans. Ind. Electron.*, vol. 58, no. 10, pp. 4746–4752, Oct. 2011.

[8] S. Cheon, Y.H.Kim, S.Y. Kang, M. L. Lee, J.M. Lee, and T. Zyung, "Circuit model based analysis of a wireless energy transfer system via coupled magnetic resonances", *IEEE Trans. Ind. Electron.*, vol. 58, no. 7, pp. 2906–2914, Jul. 2011.

[9] A. P. Sample, D. A.Meyer, and J. R. Smith, "Analysis, experimental results, and range adaptation of magnetically coupled resonators for wireless power transfer", *IEEE Trans. Ind. Electron*., vol. 58, no. 2, pp. 544–554, Feb. 2011.

[10] J. A. Ricano, H. Rodriguez Torres, H. Vazquez Leal and A. Gallardo del Angel, "Experiment about wireless energy transfer", *1-st International Congress on Instrumentation and Applied Sciences*, Cancun, Mexico, October 26-29, 2010, p.1-10.

[11] D. Niculae, Lucia Dumitriu, M. Iordache, A. Ilie, L. Mandache, "Magnetic resonant couplings used in wireless power transfer to charge the electric vehicle batteries", *Bulletin AGIR*, No. 4, pp. 155-158, 2011.

[12] A. J. Moradewicz and M. P. Kazmierkowski, "Contactless energy transfer system with FPGA-controlled resonant converter", *IEEE Trans. Ind. Electron.*, vol. 57, no. 9, pp. 3181–3190, Sep. 2011.

[13] J. I. Agbinya (Editor), *Wireless Power Transfer*, 2nd edition, River Publishers Series in Communications, Denmark, 2016.

[14] F. Zhang, X. Liu, S.A. Hackworth, R.J. Sclabassi, and M. Sun, "In vitro and in vivo studies on wireless powering of medical sensors and implantable devices", *Proc. of Life Science Systems and Applications Workshop - LiSSA*, April, 9-10, 2009, pp. 84-87.

[15] Y. Tak, J. Park, and S. Nam, "Mode-based analysis of resonant characteristics for near-field coupled small antennas", *IEEE Antennas Wireless Propag. Lett.*, vol. 8, pp. 1238–1241, Nov. 2009.

[16] C. S. Tang, Y. Sun, S. K. Nguang, and A. P. Hu, "Determining multiple steady-state ZCS operating points of a switch-mod contactkess power system", *IEEE Trans Power Electron*., vol. 24, no. 1-2, pp. 416-425, Jan.-Feb. 2009.

[17] M. Iordache, L. Mandache, D. Niculae, and L. Iordache (Bobaru), „On exact circuit analysis of frequency splitting and bifurcation phenomena in wireless power transfer systems", *Proc. of the International Symposium on Signals, Circuits and Systems - ISSCS 2015*, 9 - 10 July, 2013, Iasi, Romania, pp. 24-27.

[18] M. Iordache, A. Marinescu, I. G. Sirbu, L. Mandache, D. Niculae, and L. Iordache, "Comparative study of the frequency splitting and bifurcation phenomena for equivalent circuits of the wireless power transfer system", *Proc. of 2016 International Conference on Applied and Theoretical Electricity - ICATE*, October 6-8, 2016, Craiova, Romania, p. 1-7.

[19] C. M. Zierhofer and E. S. Hochmair, "High-efficiency coupling-insensitive transcutaneous power and data transmission via an inductive link", *IEEE Trans. Biomed. Eng*., vol. 37, no. 7, pp. 716–722, Jul. 1990.

[20] H. A. Wheeler, "Simple inductance formulas for radio coils", *Proceedings of the I.R.E.*, pp. 1398-1400, October 1928.

[21] Ansoft Q3D Extractor, *User Guide*, www.ansoft.com.

[22] E. W. Weisstein, *Quartic Equation*. From MathWorld—A Wolfram Web Resource [Online]. Available: http://mathworld.wolfram.com/QuarticEquation.html, Nov. 2011.